Mixed Disulfide with Glutathione as an Intermediate in the Reaction Catalyzed by Glutathione Reductase from Yeast and as a Major Form of the Enzyme in the Cell †

3 AUTHORS, INCLUDING:

Donna M Veine
University of Michigan
18 PUBLICATIONS   **787** CITATIONS

SEE PROFILE

Charles H. Williams Jr
University of Michigan
113 PUBLICATIONS   **4,426** CITATIONS

SEE PROFILE

Mixed Disulfide with Glutathione as an Intermediate in the Reaction Catalyzed by Glutathione Reductase from Yeast and as a Major Form of the Enzyme in the Cell[†]

L. David Arscott, Donna M. Veine, and Charles H. Williams, Jr.*

Department of Veterans Affairs Medical Center, Research Service 151, 2215 Fuller Road, Ann Arbor, Michigan 48105, and the Department of Biological Chemistry, University of Michigan, Ann Arbor, Michigan 48109

ABSTRACT: Glutathione reductase catalyzes the reduction of glutathione disulfide by NADPH. The FAD of the reductase is reduced by NADPH, and reducing equivalents are passed to a redox-active disulfide to complete the first half-reaction. The nascent dithiol of two-electron reduced enzyme (EH_2) interchanges with glutathione disulfide forming two molecules of glutathione in the second half-reaction. It has long been assumed that a mixed disulfide (MDS) between one of the nascent thiols and glutathione is an intermediate in this reaction. In addition to the nascent dithiol composed of Cys^{45} and Cys^{50}, the enzyme contains an acid catalyst, His^{456}, having a pK_a of 9.2 that protonates the first glutathione (residue numbers refer to the yeast enzyme sequence). Reduction of yeast glutathione reductase by glutathione and reoxidation of EH_2 by glutathione disulfide indicate that the mixed disulfide accumulates, in particular, at low pH. The reaction of glutathione disulfide with EH_2 is stoichiometric in the absence of an excess of glutathione. The equilibrium position among E_{ox}, MDS, and EH_2 is determined by the glutathione concentration and is not markedly influenced by pH between 6.2 and 8.5. The mixed disulfide is the principal product in the reaction of glutathione with oxidized enzyme (E_{ox}) at pH 6.2. Its spectrum can be distinguished from that of EH_2 by a slightly lower thiolate (Cys^{50})−FAD charge-transfer absorbance at 540 nm. The high GSH/GSSG ratio in the cytoplasm dictates that the mixed disulfide will be the major enzyme species.

Glutathione was discovered by F. G. Hopkins in 1921 (*1*). The glutathione−glutathione disulfide couple is present in most cells at a higher concentration than any other thiol/disulfide pair (*2*). Following elimination of glutathione as a hydrogen carrier to oxygen in 1922 (*3*), a consensus gradually emerged that it maintained the thiol−disulfide potential of the cytoplasm via thiol−disulfide interchange and that this was important because many enzymes were activated and deactivated via thiol−disulfide interchange (*4*). Glutathione also reduces harmful hydrogen peroxide, produced by the action of glutathione peroxidase. The glutathione−glutathione disulfide couple is maintained largely in the reduced state by glutathione reductase and the glutathione-glutathione disulfide ratio is between 20 and 1000 depending on cellular conditions (*5*).

Catalysis of cellular thiol−disulfide interchange reactions was not clear until only relatively recently, as enzymes catalyzing these interchanges, protein disulfide isomerase (PDI) in eukaryotes and DsbA in *Escherichia coli*, were discovered. In the past few years, a more complete understanding of the relationships between cellular thiol−disulfides has emerged (*6*). An important insight is that mixed disulfides are intermediates in the reactions and can accumulate (*7*−*10*). Thus,

$$R\text{-}S\text{-}S\text{-}R' + R''\text{-}SH \leftrightarrow R\text{-}S\text{-}S\text{-}R'' + R'\text{-}SH$$

$$R\text{-}S\text{-}S\text{-}R'' + R''\text{-}SH \leftrightarrow R''\text{-}S\text{-}S\text{-}R'' + R\text{-}SH$$

Attack on the disulfide by the thiolate usually favors one sulfur or the other, and this is determined chiefly by the relative electrophilicity of the two sulfur atoms in R-S-S-R′ (*10*−*16*). That is, if R and R′ impose differential electrophilicity on the two sulfurs, the disulfide bond will be polarized influencing which sulfur is attacked by the nucleophile. An extreme example of this is the mixed disulfide R-S-S-TNB, where TNB-S is 5-thio-2-nitrobenzoate and R-S is a cysteine residue within a protein. In an attack on this mixed disulfide by another cysteine residue, TNB-S⁻ will be the leaving group in almost all cases, since the nitrobenzoate is more electron withdrawing than most protein *milieux*. PDI and DsbA contain reactive thiols that participate directly in the catalysis of interchange. Thus, mixed disulfides between the enzyme and the substrate are intermediates in catalysis (*7*−*9*).

The flavoenzyme, glutathione reductase, contains a redox-active disulfide that is reduced by NADPH via the flavin, constituting the reductive half-reaction. The resulting dithiol reacts with the second substrate, glutathione disulfide, yielding two molecules of glutathione in the oxidative half-reaction. It was assumed that a mixed disulfide would be an intermediate in the oxidative half-reaction (*17, 18*). Direct evidence for the mixed disulfide was provided by X-ray crystallography using crystals soaked with glutathione (*19, 20*) and by chemical modification (*21*). Glutathione reductase belongs to the pyridine nucleotide-disulfide oxidoreductase

* To whom correspondences should be addressed: Phone: (734) 769-7100, ext 5611. Fax: (734) 761-7693. E-mail: chaswill@umich.edu.

family which includes lipoamide dehydrogenase and thioredoxin reductase. Glutathione reductase differs from the other two enzymes in that two molecules of the monothiol glutathione are produced, whereas in lipoamide dehydrogenase, the substrate is a dithiol and, in thioredoxin reductase, the product is a dithiol.

The reaction catalyzed by glutathione reductase shows ping-pong steady-state kinetics (22), but under the nonphysiological condition where the ratio of glutathione disulfide to glutathione is high, a ternary complex mechanism applies (23). In two-electron reduced enzyme (EH_2)[1] at equilibrium, a charge-transfer complex predominates; one of the nascent thiols (as a thiolate), referred to as the charge transfer or proximal thiol, is the donor, and FAD is the acceptor in this complex (24). This species can be detected by its absorbance beyond 540 nm where the oxidized and fully reduced enzyme (EH_4) has little absorbance. The other nascent thiol referred to as the interchange or distal thiol initiates the dithiol−disulfide interchange with glutathione disulfide that involves a transient mixed disulfide between glutathione and the interchange thiol (18−20).

The acid−base catalyst of the interchange, a histidine residue paired with a glutamate, is seen in the crystal structures of lipoamide dehydrogenase and glutathione reductase (25, 26). The primary function of the acid catalyst in glutathione reductase is to protonate the first departing molecule of glutathione, inhibiting the back-reaction, attack of glutathione thiolate on the mixed disulfide (21). A secondary function of the base is in the electron transfer from reduced flavin to the disulfide by stabilizing the thiolate−flavin charge-transfer complex (27). Thus, including the active center acid catalyst, there are three, closely linked, dissociable side chains in two-electron reduced glutathione reductase. These are, respectively, in the yeast, human or *E. coli* sequences: the interchange thiol, Cys^{45}, Cys^{58}, or Cys^{42}; the charge-transfer thiol, Cys^{50}, Cys^{63}, or Cys^{47}; and the acid catalyst, $His^{456'}$, $His^{467'}$, or $His^{439'}$, paired with $Glu^{461'}$, $Glu^{472'}$, or $Glu^{444'}$ (28−30).

In yeast glutathione reductase, a pK_a value of 3.7 (EH_3^+ to EH_2 transition) has been assigned to Cys^{50} based on its charge-transfer behavior in enzyme having Cys^{45} alkylated (31), and a pK_a value of 9.2 (EH^- to E^{2-} transition) has been assigned to the acid−base catalyst, $His^{456'}$, from both absorbance and kinetic properties (31, 32). The EH_2 to EH^- transition of yeast enzyme could be associated with pK_a values of 6.2−8.4 (18, 31−34). The pK_a values associated with glutathione reductase have been summarized (24, 34). The three groups have pK_a ranges that vary widely. While lipoamide dehydrogenase cycles in catalysis only between E_{ox} and EH_2 (35), glutathione reductase from yeast cycles either between E_{ox} and EH_2 or, less efficiently, between E_{ox} and EH^-.[2]

The high ratio of glutathione to glutathione disulfide in the cell suggests that the mixed disulfide may be a major form of the enzyme. We have therefore sought to evaluate

potential accumulation of the mixed disulfide in a study of the reaction of two-electron reduced glutathione reductase, EH_2 with glutathione disulfide, as well as the back reaction of E_{ox} with glutathione. In an effort to better understand the acid−base dynamics, we have investigated the equilibria as a function of pH.

MATERIALS AND METHODS

Materials. Yeast glutathione reductase was prepared as previously described (34). GSH, free acid, and GSSG were purchased from Sigma. All other reagents were of the highest quality available.

Solutions. The buffers have been described (34). Enzyme concentrations were 12−45 μM. Concentrated stock of yeast enzyme was stored in 25 mM Na/K phosphate, 0.3 mM EDTA, pH 7.6. Large supplies were kept frozen. Changes to the desired pH and buffer concentrations were made either by diluting a highly concentrated stock of enzyme with the desired buffer or by passage through a Bio-Rad Bio-Gel P-6DG desalting column equilibrated with the desired buffer. GSH, free acid form, was dissolved in the desired buffer then titrated to the same pH as the enzyme using NaOH. Quantitation of the thiol titer was determined using DTNB. GSSG in the GSH solutions varies from prep to prep but is always less than 2%; it was not removed. This GSSG was shown to have very little influence on the subsequent experiments. Solutions of GSSG were dissolved in the desired buffer.

Reduction of Glutathione Reductase with GSH ± GSSG. Oxidized enzyme was added to a cuvette having a syringe port, and a stopcock and the solution was made anaerobic using alternating cycles of vacuum and nitrogen (36). A gastight Hamilton syringe was used to add an appropriate concentrated solution of anaerobic GSSG into the enzyme solution. A separate solution of GSH ~50−100 equiv/20 μL was also made anaerobic and was titrated into the enzyme/GSSG mixture. The mixture was allowed to equilibrate between additions. Equilibration was determined by following the absorbance change at 540 nm until no further change could be detected. A Perkin-Elmer Lambda 6 UV spectrophotometer was used to monitor the reaction at 20 °C.

Oxidation of Two-Electron Reduced Glutathione Reductase with GSSG ± GSH. Yeast glutathione reductase was reacted with a 50-fold excess of DTT for 30 min, then applied to a 2 × 24.5 cm Sephadex G-25 desalting column equilibrated in the desired buffer to remove the excess thiol reagent. The concentration of reduced enzyme was determined from the extinction of the free FAD following guanidinium chloride denaturation. Extinction values for full EH_2 formation were derived from previous dithionite titrations (18), and the ϵ_{540nm} for E_{ox} was taken to be 200−300 M^{-1} cm^{-1}. Samples of DTT-reduced enzyme were monitored for aerobic stability for 48 h in a separate experiment and showed only minor reoxidation. Glutathione reductase from yeast has the lowest oxidase activity among the enzymes of this family (24). Titrations were performed under anaerobic conditions as described for the reductive half-reaction modified such that an appropriate concentrated solution of anaerobic GSH was titrated into the reduced enzyme prior to titration with GSSG. Oxidized glutathione was added at ~1 equiv/10 μL.

*Redox Potential of the Glutathione−Glutathione Disulfide Couple.* A wide range of values exist in the literature for

---

[1] Abbreviations: GR, glutathione reductase; GSH, glutathione; GSSG, glutathione disulfide; E_{ox}, oxidized enzyme; MDS, enzyme mixed disulfide with glutathione; EH_2, two-electron reduced enzyme; EH_4, 4-electron reduced enzyme; DTT, dithiothreitol; DTNB, 5,5'-dithiobis-(2-nitrobenzoic acid); SVD, singular value decomposition.

[2] Veine, D. M., Arscott, L. D., and Williams, C. H., Jr., unpublished results.

this redox couple. These have been "analyzed in retrospect" (*24*). We used a value of -234 mV at pH 7.0 and 20 °C. We have also used a value of 1.4 mV/°C for the standard hydrogen electrode to correct from the temperature of measurement to 20 °C (*37*). We are not aware of any systematic study of the influence of temperature on thiol–disulfide systems; a more extensive discussion of this deficiency will be found in Lennon and Williams (*38*).

Data Analysis. Spectral analysis of titrations were performed using a singular value decomposition (SVD) algorithm provided in SPECFIT software, a product of Spectrum Software Associates, Chapel Hill, NC.

Equilibrium and Model Equations. For Scheme 1,

Scheme 1

$$E_{ox} + 2GSH \xleftrightarrow{K_{-eq}} EH_2 + GSSG$$
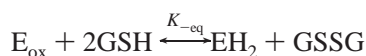
the eqs 1–4 are employed, where eq 1 is the equilibrium expression for the half-reaction of glutathione reductase with glutathione. The minus sign associated with the above equilibrium constant signifies the reverse physiological reaction; the absence of a minus sign indicates that the physiological half-reaction is under consideration (reoxidation of EH_2 with GSSG). Thus: $K_{-eq} = 1/K_{eq}$. $[GSH_i]$ and $[GSH]$ are the initial and free equilibrium concentrations of GSH, respectively. The amount of GSSG formed is assumed to be equal to the amount of EH_2 formed.

$$K_{-eq} = \frac{[EH_2][GSSG]}{[E_{ox}][GSH]^2} \tag{1}$$

$$[GSH] = [GSH_i] - 2[GSSG] \tag{2}$$

$$[E_t] = [E_{ox}] + [EH_2] \tag{3}$$

The observed extinction at 540 nm, $\epsilon_{540nm,obs}$, contains a small contribution from E_{ox} and a large contribution from EH_2.

$$\epsilon_{540nm,obs} = [\epsilon_{540nm,E_{ox}}(E_{ox}/E_t)] + [\epsilon_{540nmEH_2}(EH_2/E_t)] \tag{4}$$

For Scheme 2,

Scheme 2

$$E_{ox} + GSH\text{-}I \xleftrightarrow{K_{-2}} MDS$$

$$MDS + GSH\text{-}II \xleftrightarrow{K_{-1}} EH_2 + GSSG$$
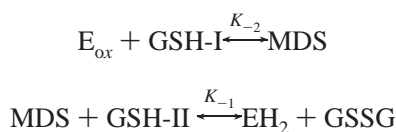
a mixed-disulfide (MDS) forms as a discrete intermediate species between E_{ox} and EH_2 and is the intermediate in the dithiol–disulfide interchange between Cys^{45} and GSSG. GSH-I and GSH-II are from the nomenclature of Pai and Schulz (*19*). GSH-I is bound on the same monomeric unit as Cys^{45}. GSH-II, however, is seen in the crystal structure to be primarily bound via salt linkages with residues on the adjacent monomeric unit at the interface of the two monomers. As with any pair of reactions having a common intermediate, MDS, the following equilibria are linked:

$$K_{-2} = \frac{[MDS]}{[E_{ox}][GSH]} \tag{5}$$

$$K_{-1} = \frac{[EH_2][GSSG]}{[MDS][GSH]} \tag{6}$$

The product of K_{-2} and K_{-1} yields an $_{app}K_{-eq}$ for the reductive half-reaction of Scheme 2, and its value may or may not equal K_{-eq} of Scheme 1, this being apparent only after the appropriate models have been evaluated.

$$K_{-2}K_{-1} = {}_{app}K_{-eq} \tag{7}$$

$$[E_t] = [E_{ox}] + [MDS] + [EH_2] \tag{8}$$

The concentration of GSH total is equal to the amount of GSH added plus the amount of MDS and EH_2 calculated. The amount of [GSSG] total, for example, as seen on the *x*-axis of Figure 5, is equal to the amount of GSSG added plus the amount of E_{ox} and MDS calculated. The amount of GSSG free, on the other hand, for the inclusion into the common denominator in eqs 9–11 (below) is computer generated from 0 to 300 μM for 100 data points which covers the entire spread of the titration experiment. Using eq 8 to solve for the equilibrium concentration of each species from eq 5 and 6, yields eq 9–11, where the common denominator is equal to

$$\{GSH + [GSSG/(GSH \times K_{-1}K_{-2})] + (GSSG/K_{-1})\}$$

$$[E_{ox}] = \{(GSSG \times E_t)/(GSH \times K_{-1}K_{-2}\}/\text{Denominator} \tag{9}$$

$$[MDS] = \{(GSSG \times E_t)/K_{-1})/\text{Denominator} \tag{10}$$

$$[EH_2] = \{GSH \times E_t\}/\text{Denominator} \tag{11}$$

$$\epsilon_{540nm,obs} = [\epsilon_{540nm,E_{ox}}(E_{ox}/E_t)] + [\epsilon_{540nm,MDS}(MDS/E_t)] + [\epsilon_{540nm,EH_2}(EH_2/E_t)] \tag{12}$$

For eq 12 to be useful, the assumption is made that the spectra of MDS and EH_2 can be distinguished.

RESULTS

Reduction of Glutathione Reductase with GSH $\pm$ GSSG. The physiological product of the reaction catalyzed by glutathione reductase, glutathione, is also capable of reducing oxidized enzyme (E_{ox}) (*22*, *24*). Figure 1 shows typical titrations of oxidized glutathione reductase with GSH, at pH 6.3 and 8.4, respectively. An increase in absorbance at 540 nm appears, indicating the formation of the thiolate–FAD charge-transfer complex, the predominant species in two-electron reduced enzyme, EH_2 (Scheme 3, species I). Since the donor of the charge-transfer interaction is a thiolate, the extinction coefficient of the complex is pH dependent as seen by comparing the two titrations (*18*, *31*). The four isosbestics in the spectra for the low pH titration indicate that there are only two species present. However, in the titration at pH 8.4, the isosbestic at 353 nm is not maintained, and this suggests the presence of an intermediate, perhaps a mixed disulfide (MDS).

The analysis that follows will show that Scheme 1 (lacking a MDS) is inadequate to describe the data even at low pH. A plot of the extinction values at 540 nm vs [GSH] shown in Figure 2, panels A and B (closed circles) conforms to a
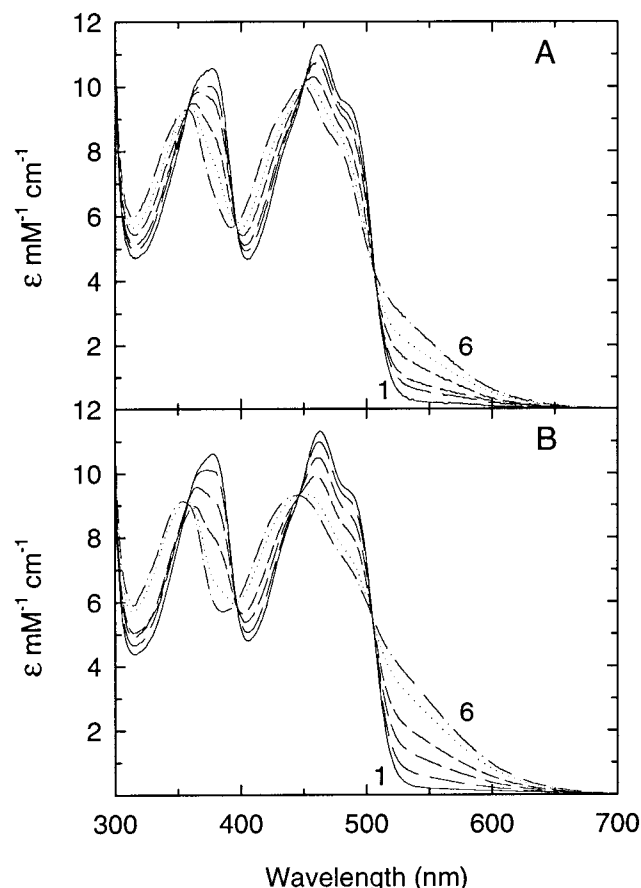
FIGURE 1: Titration of oxidized yeast glutathione reductase with GSH at pH 6.3 and 8.4. (A) The buffer was 70 mM Na/K phosphate, 0.3 mM EDTA, pH 6.3, 20 °C. The GSH concentration (mM) added to 18 μM E_{ox} was as follows: curves 1, 0; 2, 0.096; 3, 0.19; 4, 0.57; 5, 1.32; 6, 7.56. (B) The buffer was 70 mM Tris/HCl, 0.3 mM EDTA, pH 8.4, 20 °C. The GSH concentration (mM) added to 24 μM E_{ox} was as follows: curves 1, 0; 2, 0.17; 3, 0.50; 4, 1.16; 5, 3.23; 6, 7.52.
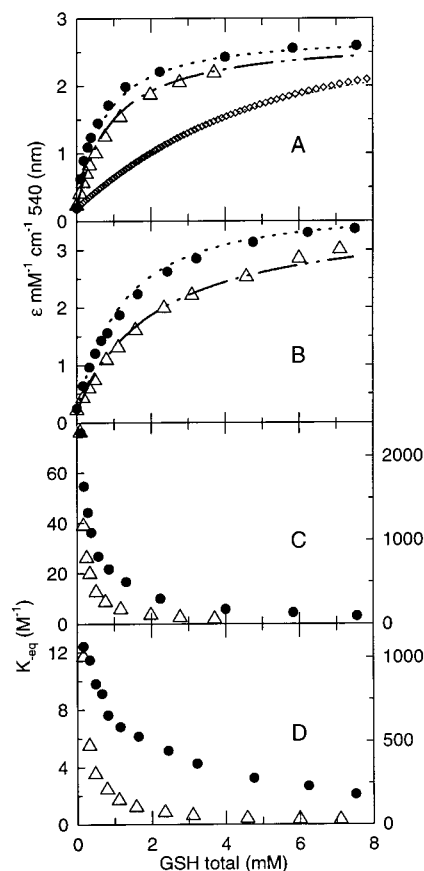

FIGURE 2: Observed increase in 540 nm extinction coefficient upon titration with GSH, in the absence and in the presence of GSSG. (A) Conditions were as in Figure 1A; data: closed circles, no GSSG; open triangles, 200 mM GSSG. The curve represented by small open diamonds shows for comparison the expected theoretical titration using Scheme 1 with a K_{-eq} of 0.79 M^{-1}. (B) conditions were as in Figure 1B; data: closed circles, no GSSG; open triangles, 395 mM GSSG. The dotted and dash−dot lines in both panels A and B were modeled using Scheme 2 as explained in the text and associated eq 5−12. (C) K_{-eq} was evaluated for both titrations in panel A using Scheme 1 with eq 1−4. (D) shows the same type of evaluation for both titrations in panel B. Both panels C and D demonstrate the inadequate description of the experimental data using Scheme 1. Note that the closed circles in panels C and D use the left-hand ordinate and that the open triangles use the right-hand ordinate.

rectangular hyperbola (fitting not shown) (*39*). It is assumed that the MDS has absorbance due to the thiolate−FAD charge-transfer complex (Scheme 3, species V). The extinction coefficient maximum calculated from this hyperbola could then, a priori, contain contributions from the MDS and from EH_2 (species I) (as well as a small contribution from E_{ox}). The fact that isosbestics are observed in these titrations suggests that the spectra of EH_2 and MDS are very similar (see below). The extinctions at 540 nm for 11 similar titration experiments, ranging in pH from 6.0 to 9.4, were almost the same (average 2.0 ± 7.2% higher) as those determined by dithionite reduction, indicating both that these reductions give rise to similar pH profiles and that, at high GSH concentration, EH_2 is fully formed (*18*). The extinction coefficients and equilibrium constants given in Table 1 have been optimized to give the best fit in various models, but the extinction coefficients differ from those determined in the GSH and dithionite titrations by less than 4% except at pH 7 where the deviation is 10%. The lower curves in both panels A and B of Figure 2 (open triangles) are for titrations done in the presence of 200 and 390 μM GSSG, for the pH values of 6.3 and 8.4, respectively. As expected, more GSH is required to approach the same extinction values as those observed in the absence of GSSG. Clear isosbestic points were observed in titrations similar to those observed in the

upper curves of Figures 1A and 2B, suggesting that no new or different species other than E_{ox} and MDS or EH_2 or both are present (data not shown).

Using the E_{m7} for E_{ox}/EH_2 of −237 mV at 20 °C for glutathione reductase from yeast (*34*) and the E_{m7} −234 mV at 20 °C for the glutathione−glutathione disulfide couple (*24*), the ΔE_m of −3 mV for the redox equilibrium of Scheme 1 and eq 1 predicts a K_{-eq} of 0.79 M^{-1} at pH 7. The redox potential for glutathione reductase was determined relative to the well-established NAD^+−NADH couple in order to avoid known complexes between EH_2 and NADPH or $NADP^+$ and to avoid MDS (*34*). Evaluation of K_{-eq} using Scheme 1 and eqs 1−4 for each titration point in Figure 2, panels A and B, is shown in panels C and D (closed circles). It can be seen that K_{-eq} is not constant. This is true at both pH 6.3 and 8.4 and also in the presence of GSSG (shown as open triangles). Moreover, at no point in the titration in the absence of GSSG is the apparent equilibrium constant near the predicted K_{-eq} of 0.79 M^{-1}. A theoretical curve, generated

Scheme 3: Intermediates in the Oxidative Half-Reaction[a]

I   II   III   IV

VIII   VII   VI   V
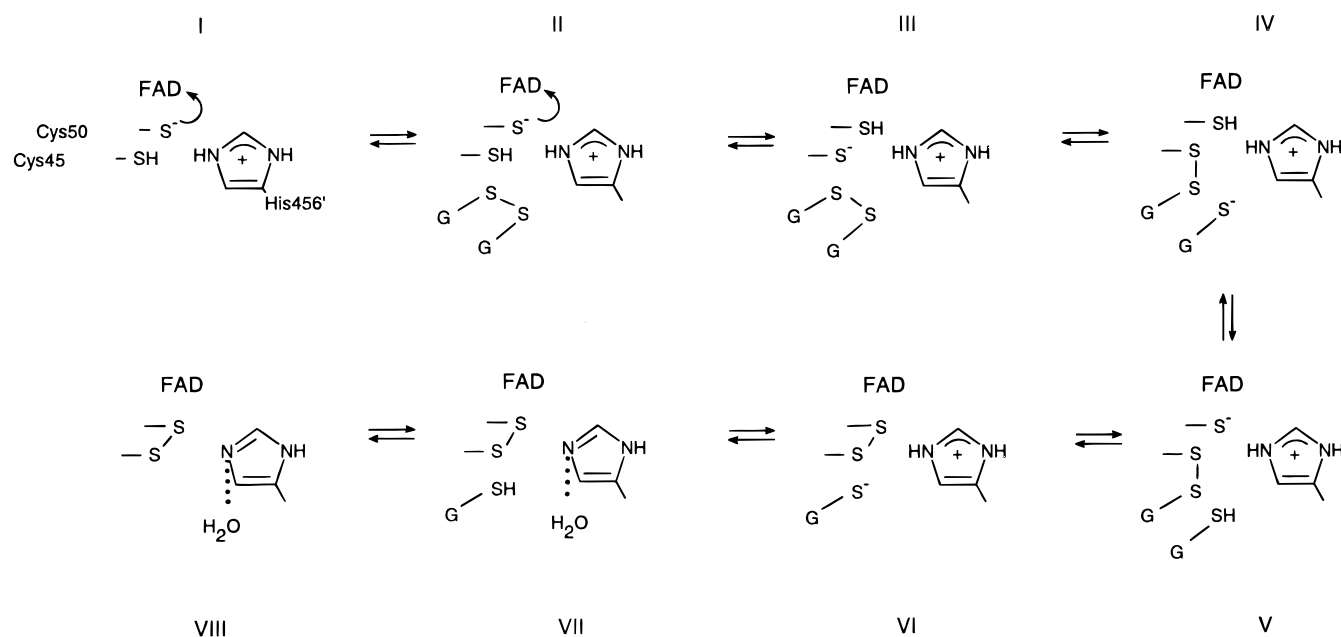
[a] Species I is the thiolate-FAD charge-transfer complex. Species IV and V are the mixed disulfide. A water molecule is hydrogen bonded to imidazole N3 in oxidized enzyme *(20)*.

Table 1: Values for Individual Extinction Coefficients and Equilibrium Constants Used to model the observed titrations of Figures 2, panels A and B, and 5, panels A−C[a]

$$EH^- H^+ + {_1}GSSG_2 \xrightleftharpoons{K_1} {_1}GS\text{-}MDS^-H^+ + {_2}GS^-H^+$$

$$_1GS\text{-}MDS^-H^+ \xrightleftharpoons{K_2} E_{ox} + {_1}GS^-H^+$$

pH	[GSH] (μM)	EH$_2$	MDS	E$_{ox}$	K_1	K_2 (M)	$_{app}K_{eq}$ (M)	$_{pH}K_{eq}$ (M)
		ϵ 540 nm (M^{-1} cm^{-1})				
6.2	100−8000	2650	2000	206	170	0.0005	0.085	0.097
7.0	540	2800	2200	206	170	0.0004	0.068	0.085
8.5	510 & 1000	3650	2200	206	170	0.0005	0.085	0.074

$$E_{ox} + {_1}GS^-H^+ \xrightleftharpoons{K_{-2}} {_1}GS\text{-}MDS^-H^+$$

$$_1GS\text{-}MDS^-H^+ + {_2}GS^-H^+ \xrightleftharpoons{K_{-1}} EH^- H^+ + {_1}GSSG_2$$

pH	[GSSG] (μM)	EH$_2$	MDS	E$_{ox}$	K_{-1}	K_{-2} (M^{-1})	$_{app}K_{eq}$ (M^{-1})	$_{pH}K_{eq}$ (M^{-1})
		ϵ 540 nm (M^{-1} cm^{-1})				
6.3	0 & 200	2700	2700	206	0.0015	1100	1.65	13.56
8.4	0 & 395	3650	3500	206	0.006	500	3.0	11.76

[a] $_{pH}K_{eq}$ and $_{pH}K_{-eq}$, are equilibrium constants calculated using the pK_a values from Table 2 and eq 13−19.

using the experimental parameters and a K_{-eq} of 0.79 M^{-1} is included for comparison in Figure 2A (small open diamonds). This curve (plotted versus GSH rather than GSH^2 for comparison) yields an apparent K_{-eq} of 4.9 mM^{-1}. None of the four actual titrations shown in Figure 2, panels A and B, comes close to this theoretical curve. Thus, Scheme 1 does not describe these equilibria.

This paradoxical result could have been due to differential binding of glutathione to E$_{ox}$ or EH$_2$, but this seems unlikely in view of the very small changes in structure of the GSH-binding site upon reduction *(20)*. However, an alternate explanation is shown in Scheme 2. This model has equilibrium characteristics similar to earlier schemes incorporating mixed disulfides as intermediates *(9, 40−42)*. A MDS in glutathione reductase has not previously been considered in spectral analysis. This MDS, however, has been included as

an intermediate in the overall catalytic mechanisms *(18, 27, 32)* and seen directly by X-ray crystallography *(19, 20)*.

The reduction of oxidized enzyme by GSH is detected as the formation of the thiolate−FAD charge-transfer complex, and it is now proposed that this dithiol form of two-electron reduced enzyme (EH$_2$) is in equilibrium with the MDS which, as subsequent data indicates, has an absorbance spectrum similar to that of EH$_2$ (Scheme 3, species I and V). It will be shown that the two equilibria of Scheme 2 have different pH dependencies (*pH Dependence of the Equilibria of Scheme 2*, below; *24, 34*). The pK_a values associated with glutathione reductase will be reviewed in the Discussion.

The data in Figure 2, panels A and B, can be modeled according to Scheme 2 and eq 12. Equations 9−11 give the concentrations of the three-enzyme species needed in eq 12.
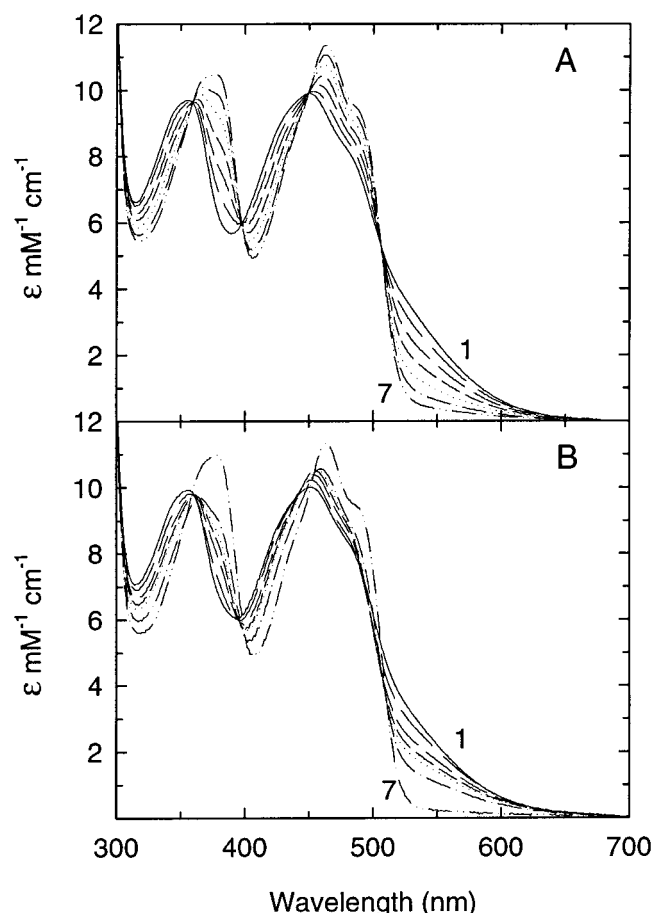
FIGURE 3: Titration of two-electron reduced yeast glutathione reductase with glutathione disulfide, (A) in the absence of GSH, and (B) in the presence of 1.08 mM GSH. The buffer was 70 mM Na/K phosphate, 0.3 mM EDTA, pH 6.2, 20 °C. (A) An equivalent of GSSG added to 20 μM EH$_2$: curves 1, 0; 2, 0.15; 3, 0.31; 4, 0.46; 5, 0.61; 6, 0.77; 7, 1.08. (B) An equivalent of GSSG added to 18 μM EH$_2$: curves 1, 0; 2, 0.17; 3, 0.5; 4, 1.0; 5, 3.0; 6, 15.1; 7, cf. E$_{ox}$.

The values used for K_{-1} and K_{-2} and the 540 nm extinction coefficients used for species, EH$_2$, MDS, and E$_{ox}$ are given in Table 1. The modeled lines are overlaid on the data, and it can be seen that fits are good. It is important to note that the equilibria of Scheme 2 are linked. Therefore, the equilibrium constants may not give a simple qualitative feeling for the position of the equilibrium.

Oxidation of Two-Electron Reduced Glutathione Reductase with GSSG $\pm$ *GSH.* Yeast glutathione reductase has a very low oxidase rate. This property allows EH$_2$ to be prepared by reduction with DTT and the excess reagent removed using an aerobic column. DTT reduces the enzyme to the EH$_2$ state and not to EH$_4$. A representative spectral titration of EH$_2$ with GSSG in the absence and presence of 1.08 mM GSH is shown in panels A and B of Figure 3, respectively, the former showing a clear set of isosbestic points and the latter showing three isosbestics that do not include the last point in the titration or the spectrum of E$_{ox}$, suggesting the presence of a MDS intermediate. Titrations of EH$_2$ with GSSG in the absence of added GSH show stoichiometric reoxidation at pH 6.3 and substoichiometric, biphasic reoxidation at pH values of 7.0 and 8.5 as shown in Figure 4. The two substoichiometric, biphasic titrations are not fully understood, but the stoichiometry may arise from the fact that the
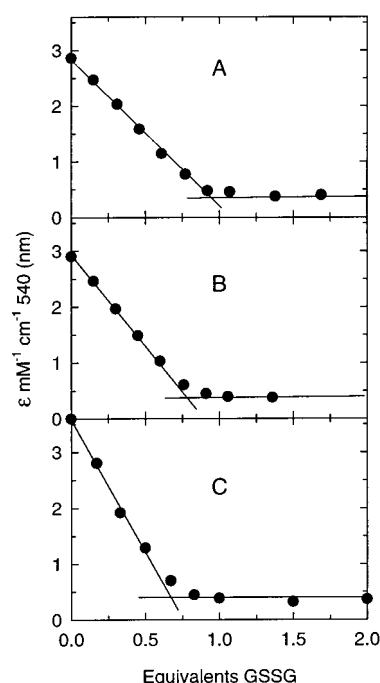

FIGURE 4: Observed decrease in the 540 nm extinction coefficient upon titration of two-electron reduced yeast glutathione reductase with GSSG, in the absence of GSH. (A) pH 6.2, conditions as in Figure 1A. (B) pH 7.0 and (C) pH 8.5.

extinction coefficient of the observed thiolate−flavin charge-transfer complex changes with pH (Figure 4, panels B and C). Thus, depending on the pH, the extinction at 540 nm may reflect different ratios of MDS and EH$_2$, (see Figure 9 and Table 1). Alternatively, as suggested by a reviewer, the quantitation of the GSSG may be inaccurate.

To establish equilibrium conditions, varying amounts of GSH were added to EH$_2$ prior to titrating the mixture with GSSG (Figure 5). In the presence of increasing concentrations of GSH, a biphasic titration results, in which the first phase appears close to stoichiometric at the low concentrations of GSH but the amount of the first phase becomes less as the concentration of GSH increases (Figure 5A, curves 5 to 1). A further gradual loss in extinction is observed with the addition of up to 10−12 equiv of GSSG. Control titrations of EH$_2$ with GSH show only a very small reoxidation due to contaminating GSSG, followed by rereduction to near 100% EH$_2$ (data not shown). Evaluation of the data in Figure 5, using Scheme 1, only in the reverse (physiological) direction, gives values for K_{eq}, which have no discernible pattern (data not shown) just as was found in the analysis of data for the reaction in the opposite direction.

Scheme 2 incorporates a MDS as an intermediate. The observed data of Figure 5 can be overlaid with model curves, using eq 12. The reciprocal of eqs 9−11 give the concentrations of the three enzyme species needed in eq 12. The values used for K_1 and K_2 and the 540 nm extinction coefficients used for species, EH$_2$, MDS, and E$_{ox}$ are given in Table 1. These model overlays do not match the data as well as those in Figure 2. This is due to the fact that eqs 9−11 require the concentration of GSSG free in solution, and this parameter cannot be determined experimentally. The match in curve 1 is better than that in curve 5, because in curve 1, very little of the added GSSG reacts so that GSSG free is essentially equal to GSSG added. The values for K_1 and K_2 in Table 1
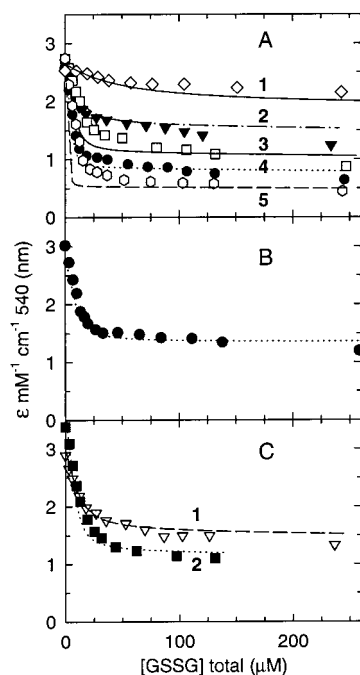
FIGURE 5: Observed decrease in the 540 nm extinction coefficient upon titration of two-electron reduced yeast glutathione reductase with GSSG, in the presence of varying concentrations of GSH and at three pH values. The EH_2 concentration was ca. 20 μM. (A) pH 6.2, conditions as in Figure 3. The GSH concentration (mM): curves 1, 8.0; 2, 1.08; 3, 0.50; 4, 0.28; 5, 0.11. (B) pH 7.0, conditions as in Figure 3. The GSH concentration was 0.54 mM. (C) pH 8.5; the buffer was as described in the Materials and Methods. The GSH concentration (mM): curves 1, 1.0; 2, 0.51. The lines overlaying the data are modeled as explained in the text and associated eq 5−12, using equilibria values and extinction coefficients from Table 1.

are not equal to the reciprocal of K_{-1} and K_{-2}, suggesting an inadequacy in Scheme 2 that does not consider the protonation state of the various enzyme species. The presence of ionizable groups near the FAD affect this facile redox equilibrium and will be discussed later.

Spectral Analysis. The spectral data for the titration of EH_2 with GSSG in the absence and presence of GSH (e.g., Figure 3) were originally analyzed by creating a set of difference spectra, subtracting the spectrum of each equilibrium mixture from the spectrum of EH_2. These had a maximum at 524 nm and minima at 462 and 492 nm. The five difference spectra at the beginning of the titration constituted a subset having two tight isosbestics; the final six difference spectra formed a distinct subset with two good isosbestics; a single difference spectrum in the middle of the titration did not fit with either subset. These data clearly show the presence of an intermediate in the conversion of EH_2 to E_{ox}, presumably MDS. However, the presence of one or more difference spectra that do not fit either subset indicates that the spectrum of MDS cannot be derived from this analysis. Indeed, a different "MDS spectrum" was derived from the data for each level of GSH, and this analysis showed that the A_{462}/A_{492} ratio changed in a characteristic fashion (see below).

Singular value decomposition (SVD) is a more rigorous tool for spectral analysis, especially for the analysis of kinetic data, e.g., A going to C via B where the spectra of A and C are known and SVD produces the spectrum of B (43). Indeed, SVD analysis of the spectra obtained during rapid (kinetic) reoxidation of *Plasmodium falciparum* glutathione reductase
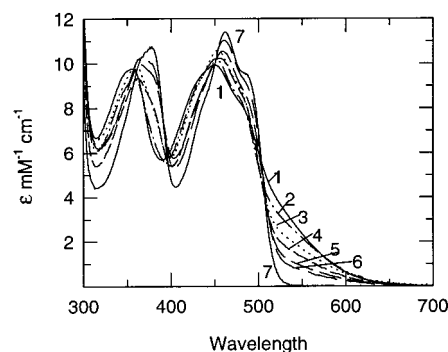

FIGURE 6: Spectral intermediates derived by SVD analysis from the titration of two-electron reduced yeast glutathione reductase with GSSG, in the presence of varying concentrations of GSH. The conditions were as in Figure 5A, pH 6.2. The GSH concentration (mM): curves 1, starting EH_2; 2, 8.0; 3, 1.08; 4, 0.50; 5, 0.28; 6, 0.11; 7 cf. E_{ox}.

by GSSG ± GSH does give a spectrum for the putative MDS which is also dependent on the GSSG/GSH ratio (44).[3] The spectra from the titration experiments used for Figure 5 were analyzed by SVD giving three unique spectral eigenvectors for each experiment. The first spectral eigenvector was that of the starting species (in this case of EH_2) while the third spectral eigenvector had the general characteristics of E_{ox}. The problem with this type of analysis is best illustrated in Figure 3B, where the last spectrum in the experiment, number six, is in the presence of 1.08 mM GSH and ca. 270 μM GSSG and can be seen to still have significant absorption due to the remaining mixture of EH_2 and MDS species. Thus, at these very high levels of GSH, there is very little E_{ox} for the SVD to take into account even at this very high level of GSSG.

The intermediate (second spectral eigenvector) had continuously changing spectral characteristics, being similar to EH_2 at high concentrations of GSH and appearing more like E_{ox} at low GSH levels. Figure 6 shows the second spectral eigenvectors derived from SVD analysis for each titration experiment of Figure 5A curves 1−5. It can be seen that the extinction at 540 nm decreases smoothly as the GSH concentration is lowered (curves 2−6). The changes at 462 and 492 nm were more complex.

Changes in the ratio of A_{462}/A_{492}, as a function of GSSG added, observed during the course of each titration are shown in Figure 7 and demonstrate clearly the formation of this MDS intermediate. EH_2 and E_{ox} have A_{462}/A_{492} ratios of 1.31 and 1.24, respectively, shown as dotted lines in Figure 7. Curve 6 shows a near linear decrease in this ratio for the experiment without added GSH (Figure 3A), demonstrating that EH_2 is converted to E_{ox} stoichiometrically. Note that even though a MDS forms under these conditions, the equilibrium favors E_{ox}. The A_{462}/A_{492} ratio changes in two phases when GSH is added at the beginning of the titration. The ratio increases (or remains level) as the first equivalent of GSSG is added (Figure 7, curves 5−1) and decreases (or increases less steeply at the highest level GSH) as the GSSG concentration is increased. This biphasic behavior is indicative of the formation of an intermediate, namely, MDS. If the highest value of A_{462}/A_{492} reached in each GSSG titration

[3] Böhme, C., Arscott, L. D., Schirmer, R. H., Becker, K., and Williams, C. H., Jr., unpublished results.
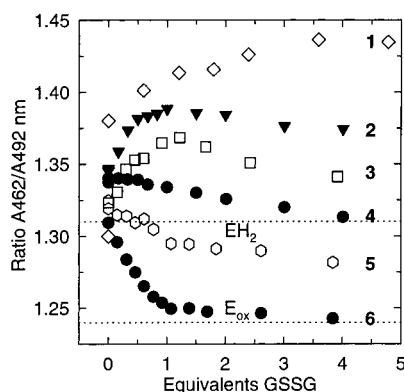
FIGURE 7: Spectral ratio A462/A492 nm observed on titration of EH$_2$ with GSSG in the absence and presence of GSH, pH 6.2. Experimental conditions were as in Figures 3A and 5A. The dotted lines indicate the ratio for EH$_2$ and E$_{ox}$ in the absence of MDS. The GSH concentration (mM): data sets 1, 8.0; 2, 1.08; 3, 0.50; 4, 0.28; 5, 0.11; 6, 0.

is plotted against the concentration of GSH (data not shown), the hyperbolic curve can be extrapolated to indicate a maximum A_{462}/A_{492} ratio of 1.45 for MDS.

pH Dependence of the Equilibria of Scheme 2. Macroscopic pK_a values associated with glutathione reductase have been determined from spectral, steady-state kinetic and redox data and are summarized in the Discussion. As mentioned above, the values for K_1 and K_2 are not equal to the reciprocal of K_{-1} and K_{-2}, suggesting an inadequacy in Scheme 2 (Table 1). The pH dependencies of the equilibria have been examined using eqs 13 and 14 for the reaction of EH$_2$ with GSSG and eqs 16 and 17 for the back reaction, reduction of E$_{ox}$ by GSH. The analysis allows for one pK_a on each enzyme species as shown in Table 2. Thus, new values have been calculated for the equilibrium constants, $_{pH}K_{eq}$ applying to the oxidative equilibria and $_{pH}K_{-eq}$ referring to the reductive equilibria (Table 1, far right column); these allow a reasonable equality to be achieved between $_{pH}K_{eq}$ and $1/_{pH}K_{-eq}$ (eq 19) in the pH range 6.0–8.5. This is reasonable given that both equilibria of Scheme 2 involve forms of the enzyme and substrate that can dissociate protons in the pH range of the study (Table 1). Scheme 3 is an expansion of Scheme 2 that shows the various protonic forms of the enzyme required for each step of the interconversion of EH$_2$ and E$_{ox}$.

DISCUSSION

A mixed disulfide formed from two-electron reduced glutathione reductase and glutathione has been observed in the structure of crystals soaked with glutathione (*19, 20*) and has been postulated in most mechanisms (*18, 27, 32*). The visible absorption spectrum of a MDS species has not

previously been described. These studies demonstrate the existence of the MDS as an intermediate in both the physiological reoxidation of EH$_2$ by GSSG and in the reverse half-reaction, reduction of E$_{ox}$ by GSH. The spectrum of the MDS has characteristics so close to those of EH$_2$ that its involvement in equilibrium experiments could only recently be appreciated when the more rigorous SVD analysis of spectral data became available. Scheme 1, which does not include a MDS intermediate, was shown to be inadequate for analysis of the data.

The inclusion of MDS as a formal intermediate, allows data to be modeled using Scheme 2 and the parameters listed in Table 1. The data in Figures 2A, 2B, 5A, 5B, and 5C have been overlaid with curves that conform to Scheme 2. The correspondence of the curves to the data is better for the reduction of E$_{ox}$ by GSH (Figure 2) than for the reoxidation of EH$_2$ by GSSG (Figure 5). This is due to the fact that eqs 9–11 require the concentration of GSSG free in solution, and this parameter is better approximated in curve 1 than in curve 5 (Figure 5A). To arrive at the approximate extinction coefficient values given in Table 1, we have used SVD to define the spectral features of MDS. As the second spectral eigenvector for each titration makes evident, the ratio GSH/GSSG determines the mixture of spectral intermediates resulting from a facile equilibrium between EH$_2$, MDS, and E$_{ox}$ (Figure 6, curves 1–6). It should be noted that the 540 nm extinction coefficients required for the MDS in modeling the reoxidation of EH$_2$ with GSSG (Figure 5) are lower in magnitude than those used to model the reduction of E$_{ox}$ with GSH (Figure 2, panels A and B), at the same pH and are lower than expected for the MDS on the basis of the data in Figure 6. The reason for this is not known, but for now our model must be considered a working hypothesis which enables us to better predict the equilibria of Scheme 2.

The fact that EH$_2$, MDS, and E$_{ox}$ are in a facile equilibrium has thus far prevented the determination of the complete spectrum of MDS by SVD. However, the data in Figure 7 allow an extrapolation that gives the ratio A_{462}/A_{492} for MDS as 1.45. As mentioned in the Results, SVD analysis of the spectra obtained in the reoxidation of *P. falciparum* GR EH$_2$ by GSSG ± GSH is able to give a similar spectrum of an intermediate attributed to the MDS. (*P. falciparum* is the major causative agent of malaria and causes the most serious form of the disease.) As with the equilibrium data presented here, the spectrum of the intermediate in the kinetic experiment depends on the GSSG/GSH ratio. The spectrum is very like that of EH$_2$ with an extinction coefficient at 540 nm of 2.65 mM^{-1} cm^{-1} at the highest GSH concentration. The ratio A_{462}/A_{492} is 1.43, very similar to that of the MDS of the yeast

Table 2: Macroscopic pKa Values Used to Model the pH Dependence of the Equilibria Shown in Table 1

EH$_2$	MDS	E$_{ox}$	2GSH	1GSH
9.0/8.0[a]	8.7[a]	5.0[b]	8.9[c]	8.9[c]

[a] See text. [b] Minimum value used in analogy to lipoamide dehydrogenase (*45*). [c] From ref *46*.

$$K_{1pH} = [K_{MDS}/(K_{MDS} + H^+)][K_{2GSH}/(K_{2GSH} + H^+)]/[K_{EH2}/(K_{EH2} + H^+)] \quad (13)$$
$$K_{2pH} = [K_{Eox}/(K_{Eox} + H^+)][H^+/(K_{1GSH} + H^+)]/[K_{MDS}/(K_{MDS} + H^+)] \quad (14)$$
and also $_{pH}K_{eq} = (K_1K_{1pH})(K_2K_{2pH}) \quad (15)$
$$K_{-2pH} = [K_{MDS}/(K_{MDS} + H^+)]/[K_{Eox}/(K_{Eox} + H^+)][H^+/(K_{1GSH} + H^+)] \quad (16)$$
$$K_{-1pH} = [K_{EH2}/(K_{EH2} + H^+)]/[K_{MDS}/(K_{MDS} + H^+)][K_{2GSH}/(K_{2GSH} + H^+)] \quad (17)$$
and also $_{pH}K_{-eq} = (K_{-2}K_{-2pH})(K_{-1}K_{-1pH}) \quad (18)$
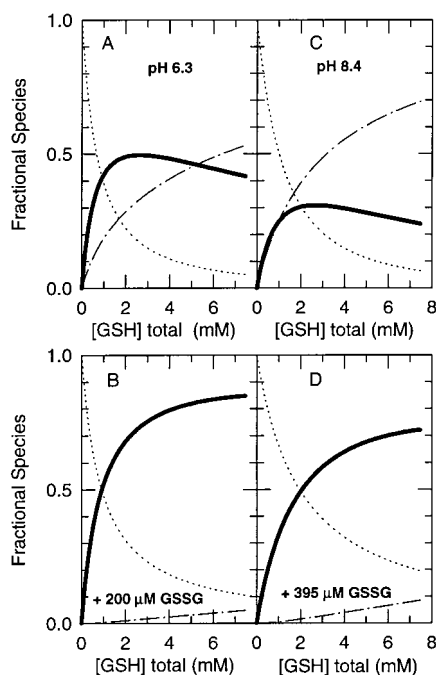$$_{pH}K_{eq} = 1/_{pH}K_{-eq} \quad (19)$$

FIGURE 8: Fractional species developed for the overlaid model curves of Figure 2, panels A and B, using parameters in Table 1. The line type indicates: dotted, E_{ox}; heavy solid, MDS; dashed—dot, EH_2.

enzyme (*44*).

Panels A—D in Figure 8 show the fraction of each species predicted from Scheme 2 for the reduction of E_{ox} by GSH; the fractions give rise to the model lines overlaying the data of Figure 2, panels A and B. It can be seen that the fraction of MDS increases when GSSG is present and decreases at higher pH.

The reoxidation of EH_2 with GSSG, in the presence of increasing concentrations of GSH, provides an interesting result recalling the biphaisic nature of the titrations (Figure 5A). Figure 9 presents similar representations of the fractional species for the predicted model curves of Figure 5A. The biphasic nature of the titrations is obvious; at GSH concentrations up to 500 μM, MDS, and E_{ox} form in the first phase with further conversion of MDS to E_{ox} in the second phase. The amount of MDS increases and there is progressively less E_{ox} as the concentration of added GSH increases.

The fact that $_{app}K_{eq}$ was not equal to the reciprocal of $_{app}K_{-eq}$ indicated that Scheme 2 was not adequate to describe

---

[4] Wong, K. K., and Blanchard, J. S., Albert Einstein College of Medicine, personal communication.

the data either at pH 6.2 or at pH 8.5 (Table 1). It should be mentioned that several other titratable residues are near the flavin and must be considered in acid—base catalysis, e.g., His[456'] is ion paired with Glu[461'] (*19*). The FAD in EH_2 is not ionized, although strongly polarized, presumably due to the charge-transfer interaction, whereas the reduced flavin in EH_4 is anionic at pH 7 (*24*). In the discussion that follows, we will focus on the three residues that participate in catalysis, the two thiols and the acid catalyst, His[456'], as shown in Scheme 3. At the EH_2 level and at neutral pH, the nascent dithiol and the acid catalyst share two protons and three protonic forms of the enzyme are possible (*34*).

Reviewing the known pK_a values, three types of data have been utilized. First, the dependence of the spectrum of EH_2 in yeast glutathione reductase on pH has been well documented (*18*, *31*); in both studies, EH_2 was generated with calibrated dithionite and subsequently titrated or rapidly mixed with buffers having higher or lower pH values. Three macroscopic pK_a values of 4.8, 7.1, and 9.2 were determined by observing the increase or decrease in absorbance at 540 nm as the pH of EH_2 was raised (EH_2 to EH^-) or lowered (EH_2 to EH_3^+), respectively. Second, several pK_a values have been derived from steady-state kinetics by Wong and Blanchard:[4] from plots of log(V/KGSSG) vs pH, pK_a values of 8.4 and 8.8 were attributed to ionizations on free EH_2 and on GSSG, respectively, and from log(*V*) vs pH, values of 6.2 and 9.2 were thought to be associated with the interchange thiol of EH_2, and the acid—base catalyst on $EH_2\cdot$GSSG, respectively. A MDS was not considered in the interpretation of these kinetic data. Finally, the dependence of the redox potential (E_{ox}/EH_2) on pH gives a pK_a of 7.4 for the yeast enzyme (*34*). The yeast enzyme has a broad pH activity optimum from pH 6.6 to 7.6 with a peak activity near pH 7 (15 000 min^{-1}/FAD) (*22*). While it is not rigorously correct to associate macroscopic pK_a values with specific groups, it can be helpful and some of these associations are based on strong spectroscopic data (*18*, *31*).

Recalling that the dithiol and the acid catalyst share two protons at neutral pH, the binding of GSSG (species I to II, Scheme 3) is assumed to shift the protonic equilibrium in favor of the interchange thiolate (species II to III) for nucleophilic attack on the substrate disulfide bond (species III to IV). On formation of the MDS (species IV), His[456'], which has become protonated in the reductive half-reaction of E_{ox} with NADPH, gives up its proton to the first departing GSH molecule, GSH-II (species IV to V). This step is crucial to prevent the back reaction of a glutathione anion attacking the newly formed MDS (*21*). His[456'] (pK_a 9.0) and Cys[50] (pK_a
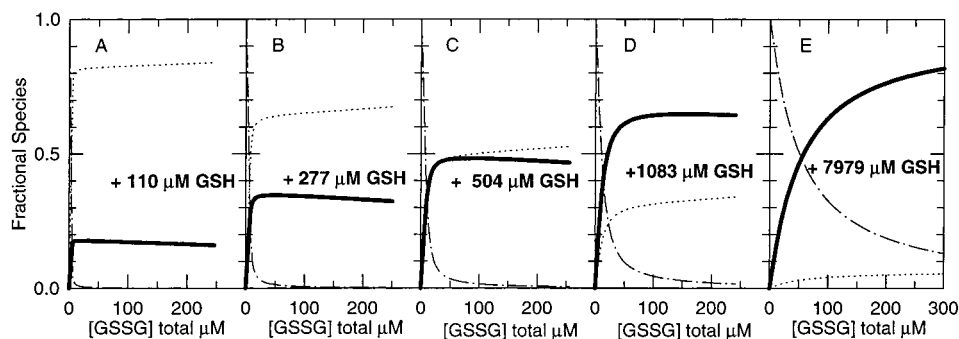

FIGURE 9: Fractional species developed for the overlaid model curves of Figure 5A curves 1—5, using parameters in Table 1. The line type indicates: dotted, E_{ox}; heavy solid, MDS; dashed—dot, EH_2.

4.8) form an ion pair and thus strongly favor proton transfer at neutral pH from Cys^{50} to $His^{456'}$ (species IV to V) setting the stage for nucleophilic attack by the thiolate of Cys^{50} on the mixed disulfide and release of the second molecule of GSH-I (species V to VI). The pK_a for $His^{456'}$ on E_{ox} is less than 5 (Table 2) by analogy with lipoamide dehydrogenase (*45*). Thus, in the reductive half-reaction of E_{ox} with GSH, it is poised to deprotonate the first GSH molecule (species VII to VI) prior to formation of the MDS (species VI to V).

Influence of pH on the Equilibria. The influence of pH on the reactions involved in thiol−disulfide interchange has been analyzed in only a very few studies (*11, 42, 47*), and relatively simple enzymes have been the object of this work. The presence of the flavin in GR is both a help and a complication. In the pH range covered by this study, which includes the physiological pH range, two pK_a values on EH_2 must be considered in its reaction with GSSG, that of the interchange thiol with a pK_a of ca. 6.2−8.4 required in its salt form (species III to IV, see above), and that of the acid−base catalyst, $His^{456'}$ having a pK_a of ca. 9.0 required in its acid form (species IV to V).

Using pK_a values for yeast GR determined in the studies described above, reasonable predictions were made for the ionization behavior of E_{ox}, EH_2, and MDS in equilibrium with GSH and GSSG in the pH range from 6.2 to 8.5 as shown in Table 2. Scheme 2, therefore, has been expanded in Scheme 3 to encompass the protonic forms of the enzyme required for each step in the reaction. Schemes 2 and 3 indicate that protons are not produced nor taken up in these reactions. This suggests that the affect of pH on these equilibria will be small. The need for expansion of Scheme 2 became apparent from the equilibrium constants for the forward and reverse reactions. The fact that $_{app}K_{eq}$ was not equal to the reciprocal of $_{app}K_{-eq}$ indicated that Scheme 2 required expansion (Table 1). Equations 13−18 in Table 2 still represent a rather simple model due to the fact that application of the acid or salt pH correction factor in any step is not obvious when two groups influence catalysis, one in the acid form and the other in the salt form. While this approach is not totally rigorous, rigor also proved elusive in the study of of DsbA [protein disulfide isomerase (*42*)]. The resulting so-called protonic equilibrium constants are presented in Table 1, $_{pH}K_{eq}$ and $_{pH}K_{-eq}$, which are approximate reciprocals (eq 19, Table 2). It can be seen that the protonic equilibrium affects primarily the reductive half-reaction of E_{ox} with GSH (lower section of Table 1). The affect of pH is observed graphically comparing Figure 8, panels A and C; at low pH where deprotonation of the enzyme and GSH is less facile, the equilibria of Scheme 3 favor the accumulation of the MDS (species IV and V) over the EH_2 (species I).

Conclusion. Evaluation of our spectral data according to Scheme 2 using SVD has allowed us to examine the spectral properties of a MDS intermediate in the reactions of E_{ox} with GSH and EH_2 with GSSG. These studies give strong support to the role of a MDS in the mechanism of glutathione reductase (*27*). It is proposed that MDS is the enzyme species that moderates the thiol/disulfide redox poise via the GSSG/GSH ratio in the cell. The graphical models aid in understanding the unique ability of GR to maintain a low concentration of GSSG in the presence of 1−10 mM cytoplasmic GSH (*5*). Reversal of the reaction species IV to

species V is unfavorable due to the pK_a values of Cys^{50} (4.8) and $His^{456'}$ (9.0) (Scheme 3). Thus, the stability of the MDS constitutes the thermodynamic barrier maintaining the high GSH concentration.

REFERENCES

1. Hopkins, F. G. (1921) *Biochem. J. 15*, 286−305.
2. Jocelyn, P. C. (1972) in *The Biochemistry of the SH Group* (Jocelyn, P. C., Eds.) pp 10−11, Academic Press, New York.
3. Dixon, M., and Hopkins, F. G. (1922) *J. Biol. Chem. 54*, 527−563.
4. Gilbert, H. F. (1990) *Adv. Enzymol. 63*, 69−172.
5. Schirmer, R. H., and Schulz, G. E. (1987) in *Coenzymes and Cofactors, Pyridine Nucleotide Coenzymes: Chemical, Biochemical and Medical Aspects* (Dolphin, D., Poulson, R., and Avramovic, O., Eds.) pp 333−379, John Wiley and Son, New York.
6. Creighton, T. E., and Freedman, R. B. (1993) *Curr. Biol. 3*, 790−793.
7. Zhang, R., and Snyder, G. H. (1988) *Biochemistry 27*, 3785−3794.
8. Darby, N. J., Freedman, R. B., and Creighton, T. E. (1994) *Biochemistry 33*, 7937−7947.
9. Darby, N. J., and Creighton, T. E. (1995) *Biochemistry 34*, 3576−3587.
10. Chivers, P. T., and Raines, R. T. (1997) *Biochemistry 36*, 15810−15816.
11. Shaked, Z., Szajewski, R. P., and Whitesides, G. M. (1980) *Biochemistry 19*, 4156−4166.
12. Wilson, J. M., Wu, D., Motiu-DeGrood, R., and Hupe, D. J. (1980) *J. Am. Chem. Soc. 102*, 359−363.
13. Snyder, G. H., Cennerazzo, M. J., Karalais, A. J., and Field, D. (1981) *Biochemistry 20*, 6509−6519.
14. Gilbert, H. F. (1989) *Biochemistry 28*, 7298−7305.
15. Chivers, P. T., Prehoda, K. E., and Raines, R. T. (1997) *Biochemistry 36*, 4061−4066.
16. Chivers, P. T., Prehoda, K. E., Volkman, B. F., Kim, B. M., Markley, J. L., and Raines, R. T. (1997) *Biochemistry 36*, 14985−14991.
17. Williams, C. H., Jr. (1976) in *The Enzymes* (Boyer, P. D., Ed.) pp 89−173, Academic Press, New York.
18. Arscott, L. D., Thorpe, C., and Williams, C. H., Jr. (1981) *Biochemistry 20*, 1513−1520.
19. Pai, E. F., and Schulz, G. E. (1983) *J. Biol. Chem. 258*, 1752−1757.
20. Karplus, P. A., Pai, E. F., and Schulz, G. E. (1989) *Eur. J. Biochem. 178*, 693−703.
21. Wong, K. K., Vanoni, M. A., and Blanchard, J. S. (1988) *Biochemistry 27*, 7091−7096.
22. Massey, V., and Williams, C. H., Jr. (1965) *J. Biol. Chem. 240*, 4470−4480.
23. Boggaram, V., Larson, K., and Mannervik, B. (1978) *Biochim. Biophys. Acta 527*, 337−347.
24. Williams, C. H., Jr. (1992) in *Chemistry and Biochemistry of Flavoenzymes* (Müller, F., Ed.) Vol. III, pp 121−211, CRC Press, Boca Raton.
25. Mattevi, A., Schierbeek, A. J., and Hol, W. G. J. (1991) *J. Mol. Biol. 220*, 975−994.
26. Schulz, G. E., Schirmer, R. H., Sachsenheimer, W., and Pai, E. F. (1978) *Nature 273*, 120−124.
27. Rietveld, P., Arscott, L. D., Berry, A, Scrutton, N. S., Deonarain, M. P., Perham, R. N., and Williams, C. H., Jr. (1994) *Biochemistry 33*, 13888−13895.

28. Collinson, L. P., and Dawes, I. W. (1995) *Gene 156*, 123–127.

29. Krauth-Siegel, R. L., Blatterspiel, R., Saleh, M., Schiltz, E., Schirmer, R. H., and Untucht-Grau, R. (1982) *Eur. J. Biochem. 121*, 259–267.

30. Greer, S., and Perham, R. N. (1986) *Biochemistry 25*, 2736–2742.

31. Sahlman, L., and Williams, C. H., Jr. (1989) *J. Biol. Chem. 264*, 8033–8038.

32. Wong, K. K., and Blanchard, J. S. (1989) *Biochemistry 28*, 3586–3590.

33. Arscott, L. D., Veine, D. M., and Williams, C. H., Jr. (1991) in *Flavins and Flavoproteins 1990* (Curti, B., Ronchi, S., and Zanetti, G., Eds.) pp 529–532, Walter de Gruyter, Berlin.

34. Veine, D. M., Arscott, L. D., and Williams, C. H., Jr. (1998) *Biochemistry 37*, 15575–15582.

35. Matthews, R. G., and Williams, C. H., Jr. (1976) *J. Biol. Chem. 251*, 3956–3964.

36. Williams, C. H., Jr., Arscott, L. D., Matthews, R. G., Thorpe, C., and Wilkinson, K. D. (1979) in *Methods in Enzymology – Vitamins and Coenzymes* (McCormick, D. B., and Wright, L. D., Eds.) pp 185–198, Academic Press, New York.

37. Clark, W. M. (1960) *Oxidation–Reduction Potentials of Organic Systems*, The Williams & Wilkins Company, Baltimore.

38. Lennon, B. W., and Williams, C. H., Jr. (1996) *Biochemistry 35*, 4704–4712.

39. Massey, V., Ghisla, S., Ermler, U., and Schulz, G. E. (1987) in *Flavins and Flavoproteins* (McCormick, D. B., and Edmondson, D. E., Eds.) pp 79–84, Walter de Gruyter and Co., Berlin.

40. Walters, D. W., and Gilbert, H. F. (1986) *J. Biol. Chem. 261*, 15372–15377.

41. Freedman, R. B., Hirst, T. R., and Tuite, M. F. (1994) *Trends Biochem. Sci. 19*, 331–336.

42. Nelson, J. W., and Creighton, T. E. (1994) *Biochemistry 33*, 5974–5983.

43. Henry, E. R., and Hofrichter, J. (1992) *Methods Enzymol. 210*, 129–192.

44. Böhme, C. C., Becker, K., Schirmer, R. H., Arscott, L. D., and Williams, C. H., Jr. (1999) in *Flavins and Flavoproteins 1999* (Ghisla, S., Kroneck, P. Macheroux, P., and Sund, H., Eds.) pp 899–902, Agency for Scientific Publication, Berlin.

45. Matthews, R. G., Ballou, D. P., Thorpe, C., and Williams, C. H., Jr. (1977) *J. Biol. Chem. 252*, 3199–3207.

46. Rabenstein, D. L. (1989) in *Coenzymes and Cofactors, Glutathione: Chemical, Biochemical and Medical Aspects* (Dalphin, D., Poulson, R., and Avramovic, O., Eds.) pp 147–3186, John Wiley and Son, New York.

47. Szajewski, R. P., and Whitesides, G. M. (1980) *J. Am. Chem. Soc. 102*, 2011–2026.